

Generative molecule evolution using 3D pharmacophore for efficient Structure-Based Drug Design

Yi He^{1,†,°}, Ailun Wang^{1,°}, Zhi Wang¹, Yu Liu¹, Xingyuan Xu¹, Wen Yan^{1,†}

¹ByteDance Seed

[†]Corresponding authors, [°]Equal Contribution.

Abstract

Recent advances in generative models, particularly diffusion and auto-regressive models, have revolutionized fields like computer vision and natural language processing. However, their application to structure-based drug design (SBDD) remains limited due to critical data constraints. To address the limitation of training data for models targeting SBDD tasks, we propose an evolutionary framework named MEVO, which bridges the gap between billion-scale small molecule dataset and the scarce protein-ligand complex dataset, and effectively increase the abundance of training data for generative SBDD models. MEVO is composed of three key components: a high-fidelity VQ-VAE for molecule representation in latent space, a diffusion model for pharmacophore-guided molecule generation, and a pocket-aware evolutionary strategy for molecule optimization with physics-based scoring function. This framework efficiently generate high-affinity binders for various protein targets, validated with predicted binding affinities using free energy perturbation (FEP) methods. In addition, we showcase the capability of MEVO in designing potent inhibitors to KRAS^{G12D}, a challenging target in cancer therapeutics, with similar affinity to the known highly active inhibitor evaluated by FEP calculations. With high versatility and generalizability, MEVO offers an effective and data-efficient model for various tasks in structure-based ligand design.

Date: July 29, 2025

Correspondence: YH at heyi@bytedance.com, WY at wen.yan@bytedance.com

1 Introduction

Drug discovery and development is a complex and iterative process. It involves designing and optimizing molecules towards sufficient affinity for specific protein targets while fulfilling stringent property requirements. Traditional drug discovery methodologies frequently employ high-throughput screening (HTS) to discover starting compounds for small-molecule drug design campaigns from a predefined library of compounds[5, 39]. To reduce the time and cost associated with the traditional HTS methods, virtual screening (VS) has been employed to facilitate fast evaluation over extensive libraries of compounds with either empirical scoring functions[15, 18, 19, 55] or machine learning models[10, 52]. Although screening methods have successfully identified many drug candidates, it is inherently limited by the chemical diversity within existing compound libraries [38]. The theoretical chemical space of drug-like molecules is enormous, estimated to range between 10^{33} and 10^{60} compounds [46], which far exceeds even the largest available chemical libraries and makes it costly and impractical to exhaust with screening methods. Limited by computing resources, inexpensive scoring functions have to be used on screening these vast virtual libraries, which lead to inaccuracies and less

generalizability due to the neglect of entropic contribution, solvation effect and protein flexibility[22, 50, 67]. However, the synthesizable chemical space has been growing rapidly and has reached trillion-molecule scale[40]. Therefore, even these rapid scoring functions cannot be naively used and some data-driven techniques[37] must be applied to shrink the candidate search space.

Deep generative models have dramatically advanced content creation, achieving remarkable results in generating high-fidelity images [48], coherent text [47], and realistic audio [56]. These successes are primarily driven by the availability of extensive, high-quality datasets, enabling generative architectures to effectively capture and internalize intricate domain-specific patterns, to generate outputs that adhere closely to physical, linguistic, or acoustic constraints.

In recent years, deep generative models have also been applied to efficiently and accurately model molecular structures, significantly enhancing exploration within chemical spaces during molecule generation. [2, 6, 9, 11, 14, 21, 25, 34, 36, 43, 44, 58, 61–65, 68] However, directly transferring these advances into practical drug design applications remains challenging. Generative models employed in ligand-based drug design (LBDD) benefit from abundant training data but typically overlook the structural context and flexibility of target binding pockets, which consequently limits their ability to design molecules with high affinity and specificity. While structure-based drug design (SBDD) methods [8, 20, 32, 45] explicitly incorporate pocket geometry, they are hindered by the limited scale, quality, and diversity of available protein-ligand structural data. Current datasets, such as the experimentally curated protein-ligand complex structures in PDB or computationally expanded datasets like HelixDock[28] and crossdocked[17], are significantly fewer than the billion-scale datasets driving advancements in vision and language modeling. High quality datasets of protein-ligand complexes with reliable affinity labels, such as PDBbind[33], are even rare with only tens of thousands of samples. Moreover, these datasets frequently suffer from limited chemical diversity [26], noisy annotations [54], and biases toward certain affinity ranges [38], which limits models’ generalizability to novel targets and chemically innovative ligand proposals.

The vast chemical space is not only a challenge for drug discovery, but also a chance for data scaling up because although the protein-ligand complex data is limited, the ligand-only data is almost unlimited. This is our motivation to develop MEVO, a novel framework combining the strengths of extensive training data in LBDD and structural awareness in SBDD, to facilitate efficient *de novo* drug design. Specifically, MEVO leverages pharmacophore-guided generative methods trained on billion-scale unsupervised molecular datasets from the Enamine REAL database [35] and ZINC20 database[27]. The extensive coverage of drug discovery chemical space in these databases enables MEVO to learn robust pharmacophore patterns from high-quality molecular conformations, facilitating the generation of diverse and plausible molecules. Additionally, we propose a novel evolutionary optimization technique that integrates pharmacophore requirements with detailed protein pocket geometry. This evolutionary approach enables iterative refinement of generated molecules based on a target-specific scoring function, progressively improving binding affinity, as confirmed through rigorous binding free energy calculations. By separating the learning of universal chemical rules (from unsupervised data) from target-specific adaptation (via evolution), our method avoids overfitting to sparse or biased protein-ligand data. This strategy uniquely equips MEVO to generate novel ligands satisfying both pharmacophore principles and target-binding constraints.

2 Results

Overview of the MEVO model

In MEVO, we utilize a discrete diffusion model to generate non-covalent ligands on targets with known protein structures and potential binding pockets. The primary goal of MEVO is to efficiently generate molecules that bind effectively to the target protein pocket with desirable affinity. To achieve this, MEVO incorporates three key components, as depicted in Figure 1:

- A Vector Quantised-Variational AutoEncoder (VQ-VAE), enabling accurate translation between molecular structure and latent tokens, thus serving as the basis for latent-space molecular generation;
- A latent diffusion model (LDM) for conditional molecule generation, which is precisely guided by protein

pocket structures and pharmacophore constraints;

- An evolutionary optimization strategy, connecting pharmacophore and pocket conditions to iteratively improve generated molecules, optimizing their binding affinity.

The 3D molecular structure comprises both categorical features such as atom and bond types, and numerical features as coordinates, posing a significant multi-modal challenges for diffusion models. To handle this complexity, we employ a VQ-VAE to unify these modals in one latent space (Figure 1B). Specifically, a molecule encoder compresses molecular structures into latent tokens, and a decoder reconstructs molecules from these tokens. We train the VQ-VAE on Enamine REAL [35], which comprises 9.6 billion synthetically feasible molecules, and supplement it with over 750 million commercially available compounds from ZINC20 [27], achieving near-lossless reconstruction accuracy. Leveraging the high-quality representations from the VQ-VAE, we train our generative diffusion model directly in the latent space, circumventing the need for feature-specific noise adjustments.

The latent diffusion model is core to MEVO’s capability of generating novel molecules. Based on Discrete Denoising Diffusion Probabilistic Models (D3PMs)[3], our latent diffusion model operates within a discrete latent space, enabling conditional generation tailored to specific pharmacophore and pocket constraints. In this model, noise is incrementally introduced to latent tokens during a forward diffusion process, and a transformer-based denoising network[57] progressively removes this noise (Figure 1A). To integrate the information from both ligand and protein, we design separate embeddings for pharmacophore conditions and pocket conditions, which are derived from the ligand and protein structures, respectively. These condition embeddings, combined with embeddings of the noisy latent tokens, serve as input to the denoising network. Using the transformer-based denoising network, the model can effectively attend to the conditioning features while denoising each latent token, such that the generated molecules fit both pharmacophore and pocket conditions.

Finally, the evolutionary strategy enhances the quality of generated molecules by incorporating a physics-informed scoring function into the generation process (Figure 1C). Further details on this evolutionary approach are provided in the following section.

MEVO enhances pocket-aware ligand design with evolutionary strategy

In drug design, it is usually not sufficient to simply fit the geometry of the designed molecule to the shape of the binding pocket. More importantly, the non-covalent binders should form favorable protein-ligand interactions (e.g. hydrogen bond, etc.), which is crucial to bind the pocket with strong affinity. Therefore, in addition to diffusion-based molecule generation and pharmacophore- and pocket-conditioned generation, we introduce an evolutionary strategy to progressively improve the affinity of generated molecules to the target protein.

Our evolutionary approach employs a physics-informed scoring function, swiftly evaluating generated molecules based on the change of potential energies upon binding (ΔU) and the fulfillment of desired protein-ligand interactions (ρ). The product of these two metrics forms a final score ($-\Delta U \times \rho$), which quantitatively measures the performance of each molecule concerning the targeted protein. Though this scoring is not as reliable as more sophisticated alchemical transformation methods such as absolute free energy perturbation (ABFEP), it can be evaluated at a computational cost close to docking scores, orders of magnitude faster than ABFEP. Furthermore, we find this simple interaction score can significantly outperform docking score in ranking potential hits. In each evolutionary generation, generated molecules are ranked according to this simple but effectively interaction score, and the top-ranking molecules serve as seed molecules, which provide additional guidance for the subsequent generation cycle. Exquisitely, the structural information of seed molecules as well as how they interact with the binding pocket are converted into pharmacophore conditions, which are used as additional conditions in the following round of molecule generation. In this manner, the evolutionary process in MEVO effectively bridges the data hunger pocket conditions with the data rich pharmacophore conditions, benefiting from extensive billion-scale training data. This integration significantly accelerates the improvement in molecular affinity with only a few evolutionary cycles. It is worth noting that there is no additional training process required for this evolutionary process, and the evolution is purely established

on the scoring function. Hence, various scoring functions can be simply incorporated into this evolutionary strategy, and we expect the model’s performance to improved if more accurate scoring functions are applied. Moreover, this training-free evolutionary strategy can be easily transferred to other tasks beyond pocket-aware ligand design targeting high affinities, it can also be applied to generative tasks focusing on optimizing other properties of ligands, such as permeability, solubility, etc.

MEVO generates drug-like molecules with desirable properties

To benchmark the overall performance of MEVO in drug design, we compare properties of molecules generated by MEVO with those of real binders. Here, we use the publicly available set of FDA-approved drugs as reference molecules to evaluate the generated molecules using widely recognized metrics: Lipinski’s rule of five (Lipinski RO5), distribution of ring sizes within molecules, quantitative estimate of drug-likeness (QED), synthetic accessibility (SA), and predicted octanol-water partition coefficient (logP).

As examples, we generated molecules targeting 5 different proteins and selected the top-50 ranked molecules from each target, resulting in a total of 250 molecules for evaluation. Reference molecules are collected from the FDA-approved drug list after sanitization using RDKit, totaling 2094 molecules. As shown in Figure 2A, most generated and reference molecules comply with Lipinski’s RO5. The distribution of ring sizes in generated molecules closely matches that of the reference set, with a slight overrepresentation of five- and six-membered rings (Figure 2B). The QED distribution (Figure 2C) indicates that generated molecules exhibit reasonable but slightly lower drug-likeness scores than reference molecules. The logP distributions (Figure 2D) for generated and reference molecules are very similar, predominantly within the optimal range of 0–5 for oral administration. Additionally, generated molecules exhibit slightly higher molecular weights compared to the FDA-approved drugs (Figure 2E), consistent with the observed higher frequency of larger rings.

Here, no restrictions or conditions are posed on MEVO in generating these molecules. However, flexible customizations can be conveniently included. For example, MEVO allows users to define desired ranges of heavy atom counts, enabling generation of molecules tailored to specific molecular weight preferences.

MEVO is efficient in hit discovery

In early stage of drug discovery, a generative model can replace a traditional virtual screening campaign in identifying a hit molecule with promising affinity to the target protein pocket. In this section, we demonstrate MEVO’s ability in discover hits from a vast chemical space conditioning on protein structures, without any prior knowledge except residues defining the target protein pocket. To show the generalizability and transferability of MEVO, we systematically benchmarked MEVO’s capability for pocket-aware ligand design on five protein targets with various sizes and shapes, which were selected from a publicly available binding free energy benchmark dataset [49, 59]. On majority of tested targets, MEVO successfully produced ligands with binding affinities comparable to or exceeding those of known binders. Moreover, the molecules generated by MEVO effectively preserved critical interactions within the binding pockets, providing a strong foundation for developing potent ligands.

To quantitatively evaluate the binding affinity of MEVO-designed ligands, we employ the rigorous free-energy perturbation (FEP) method to calculate absolute binding free energies (ABFE, $\Delta G = G_{PL} - G_P - G_L$) for the top-ranked generated molecules. The FEP method is widely recognized for its accuracy in predicting ligand-protein binding affinities consistent with experimental results. For each protein target, MEVO only takes the protein structure and protein residue indices defining the binding pocket as input, without using any fragments or scaffolds from the reference ligands, emulating a typical hit discovery scenario in drug design. From generated molecules for each target, the top-10 ranked molecules are selected to proceed into the FEP evaluation (Figure 3A). The binding affinities of reference molecules are also calculated using the same FEP method, and plotted side-by-side with the calculated affinities of generated molecules for the same target. As shown in Figure 3A, MEVO-generated molecules have binding affinities that are comparable to or superior to known binders for 4 out of the 5 tested targets. It is a promising performance of MEVO in terms of generating high affinity binders, especially considering that no human adjustments are involved during the whole generation process, and all candidate ligands are generated and optimized automatically through the molecule generation and evolution modules in MEVO. For targets on which MEVO did not generate higher

affinity binders than reference ligands, such as p38, the affinities of generated ligands can be further improved through the lead optimization process using MEVO, following the same manner illustrated in the next section regarding a case study of KRAS inhibitor design.

As a key component to the architecture of MEVO, the evolutionary strategy plays an important role in improving the quality of generated ligand candidates, especially for improving the ligand affinities to the target protein. For all the 5 target tested in this work, we collected the rounds of evolution for each high affinity binders, which spreads in the range of 10 to 50 rounds (Figure 3C). In the process of evolution, MEVO is able to generate high affinity binders which are highly different from the known reference binders, while maintaining high scaffold diversity of the generated ligands. To quantify the differences between generated molecules and reference ligands, we calculate the Tanimoto similarity between the MEVO-generated high affinity binders and the reference binders (Figure 3D), which illustrates the novelty of generated molecules. Moreover, we extract the Murcko scaffold [4] from each MEVO-generated high affinity binders and calculate the pairwise Tanimoto similarity between scaffolds associated with the same target (Figure 3E). The pairwise scaffold similarity indicates that these high affinity binders generated by MEVO for the same target are highly different from each other. As a reference for comparison, we also calculate the pairwise scaffold similarity for reference ligands for each target (Figure 3E). Since the reference ligands in this dataset are mainly obtained by R-group enumerations, which is consistent with their relatively low diversities observed here. Additionally, we compute protein-ligand interaction fingerprint (PLIF) using ProLIF [7] for both known binders and MEVO-generated molecules, then calculate the extent to which that generated ligands retain the critical interactions observed in the reference binders, using the PLIF-recovery rate defined by Errington *et al* [16] (details in Methods). To provide sufficient sampling for the protein-ligand interaction analysis, top-50 ranked ligands for each target protein are involved in the interaction recovery analysis, and the result demonstrates that MEVO successfully preserves the majority of critical interactions (Figure 3B).

MEVO provides high versatility for designing KRAS^{G12D} inhibitors

KRAS is among the most frequently mutated proteins in cancer, which plays essential roles as GTPase and transits between active (GTP-bound) and inactive (GDP-bound) states.[1, 51] Given the intracellular abundance of GTP and the extremely high (picomolar) affinity of KRAS for GTP/GDP, it is notoriously challenging to design competitive inhibitors targeting the orthosteric site in the switch-I pocket (Figure 4A)[24, 29, 41, 42]. Over the past decade, significant breakthroughs have been achieved with inhibitors targeting the switch-II pocket of KRAS (Figure 4A)[30], including both covalent and non-covalent inhibitors[13, 23, 31, 60]. As one of the pioneers in KRAS’s non-covalent inhibitors, MRTX-1133 from Mirati Therapeutics exhibits sub-piccomolar affinity ($\sim 0.2\text{pM}$) to KRAS^{G12D} and roughly 700-fold selectivity over KRAS^{WT} [23, 60]. Nevertheless, challenges persist in enhancing affinity and selectivity of KRAS inhibitors and propose more potent inhibitor candidates from the vast chemical space.

In this study, targeting the KRAS^{G12D} switch-II pocket, we leverage MEVO’s high versatility and efficiency to design high affinity binders to the switch-II binding pocket. During this process, MEVO is applied multiple times at various stages of molecule design, rendering different scenarios of drug discovery. Owing to the iterative evolution strategy in MEVO, we successfully generate several lead molecules, and further validate the affinity of MEVO-designed lead molecule using Schrödinger’s FEP+ software[12], which indicates comparable affinity to the highly active MRTX-1133 ligand.

Due to the exceptional affinity and selectivity of MRTX-1133 to KRAS^{G12D}, MRTX-1133 provides a valuable reference for designing new KRAS inhibitors. By analyzing the key interactions of MRTX-1133 with the switch-II pocket of KRAS^{G12D} (Figure 4B), a fragment is extracted from MRTX-1133 and serves as the starting scaffold for MEVO (Figure 4C, 4E, fragment 1). Starting from this fragment, MEVO is able to generate plenty of new molecules by exploring diverse regions of the switch-II pocket, which renders a ligand growing process. After examining the top-ranked molecules generated by MEVO, a novel interaction is observed between MEVO-designed ligand **1** (Figure 4E) and residue GLY-10 in a deeper region of the switch-II pocket, via a six-membered ring (Figure 4C, 4E, fragment 2). Taking both fragment 1 and 2 as input conditions, the next round of ligand design by MEVO is turned into a linker design problem. Since both fragment 1 and 2 are not interacting with the mutation site G12D, the goal of linker design is to establish stable interactions

with G12D, while preserving key interactions from the reference fragments. This goal has been successfully achieved by ligand 3, which interacts with ASP-12 by a secondary amine linker. To further illustrate the versatility of MEVO, we use it as a lead optimization tool and performed substitution enumerations on ligand 3 to further improve its binding affinity, which leads to the generation of ligand 4 (Figure 4D). As a validation, we predict the absolute binding free energy of ligand 4 to KRAS^{G12D} via rigorous ABFEP calculations using FEP+ software, yielding a value of -22.31 kcal/mol. The absolute binding free energy of ligand 4 corresponds to an estimation of K_D value around 10^{-4} pM, which is expected to have comparable activity with the highly active MRTX-1133. This result underscores the efficiency and versatility of MEVO in target-aware ligand design.

3 Conclusion

In the present study, we have developed a pocket-aware pharmacophore-guided deep learning model for *de novo* molecule generation, termed MEVO. This model synergizes the following architectures into a single framework: (1) a VQ-VAE module for accurate molecule representation in the latent space and high-fidelity molecule reconstruction, (2) a LDM for conditional molecule generation to allow for effective exploration of the chemical space, and (3) an evolutionary molecule optimization strategy to efficiently improve the binding affinity of generated molecules. This framework offers great advantages over current models for molecule generations. By elegantly bridging the data-hungry SBDD methods with the data-rich LBDD methods, MEVO effectively increases the abundance of training data for pocket-aware ligand design, and subsequently improves the quality of generated molecules. In addition to the generative model, MEVO also incorporates a carefully-designed post-processing workflow, which refines the coordinates of generated ligand molecule with the protein pockets through a force field guided structure relaxation, and reduces undesired steric clashes. Using a physics-based scoring function, MEVO is able to rapidly assess the quality of each generated molecule according to their interactions with the protein pocket, and further improve the quality of molecules using the evolutionary strategy.

Tested on various protein targets, MEVO is able to generate comparable and even higher affinity binders for the targeted binding pockets, which is validated by rigorous ABFEP calculations. Additionally, with very high versatility, MEVO can be applied to different stages in the drug design processes, as showcased in the inhibitor design for KRAS^{G12D}. By integrating the advanced deep learning methods with the physics-based scoring function, MEVO brings a comprehensive and effective tool for pocket-aware ligand design. The success of MEVO also shows the feasibility of transforming different types of data to significantly increase the abundance of training data for models, and subsequently improve the performance of the trained models. In addition to molecule design, this training-free evolutionary strategy can also be extended to other tasks, especially in tasks of structure-based predictions for biomolecules, which constantly suffer from the lack of large-scale high-quality training data. Models targeting these tasks will benefit from the improved availability of training data by applying similar strategy as in MEVO, and better performances can be expected in the future.

4 Methods

Dataset preparation

In MEVO, the Enamine REAL database[35] and ZINC20 database[27, 53] are used as sources of training data. The Enamine REAL database is a comprehensive collection of 9.6 billion compounds that are synthetically feasible, which provides a highly diverse training set for the molecule generative model. While the ZINC20 dataset encompasses over 750 million commercially-available compounds, with over 230 million compounds in ready-to-dock, 3D formats. From the source databases, for molecules with only 2D representation, the 3D conformation of each compound was generated from its 2D representation using the RDKit package. It is observed that small molecules in the Enamine REAL database have imbalanced distribution in terms of heavy atoms counts (HAC), with nearly 70% of molecules containing 20 to 30 heavy atoms. To improve MEVO’s ability of generating larger molecules, we resample the source databases to balance the HAC distribution in the training set of MEVO, ensuring a 2:3:3:2 ratio for molecules with <20, 20-30, 30-40, and 40-50 heavy atoms.

To train the conditional generation of small molecules, the HelixDock [28] dataset is also included in the training sets. In the training of pharmacophore conditional generation, the pharmacophore characteristics of small molecules from training sets, including compounds from Enamine REAL, ZINC20 and HelixDock datasets, are extracted using RDKit. For training the small molecule generation conditioned on protein pockets, the structure of protein-ligand complexes from the HelixDock dataset are used.

Molecular Representation

A 3D molecular geometry is represented by $\mathcal{G} = (\mathcal{V}, \mathcal{E}, \mathcal{X})$, where \mathcal{V} denotes the categorical features of the heavy atoms in the molecule, \mathcal{E} denotes pairwise edge features, and \mathcal{X} represents the 3D atom coordinates. The categorical atom features $v_i \in \mathcal{V}$ can be further divided into three components: $v_i = [a_i, h_i, c_i]$, where a_i, h_i, c_i are categorical features indicating atom type, hydrogen count and formal charge respectively. The pairwise edge features $e_{ij} \in \mathcal{E}$ indicate the whether there is a bond between atom i and atom j , and the bond type if present, which can be one of the following: no bond, single bond, double bond, triplet bond and aromatic bond. The 3D atom coordinate $x_i \in \mathbb{R}^3$ is extracted from the heavy atom i . In the molecular representation, only heavy atoms are explicitly represented while hydrogen atoms are implicitly represented through the combination of hydrogen counts and formal charges (-2 to +2) on the neighboring heavy atoms. Such representation significantly reduces the complexity of the molecular graph representation, while preserving chemical validity via valence constraints.

With implicit representation of hydrogen atoms in the molecule, the aforementioned molecular representation is still capable of accurately reconstructing the entire molecular structures, including the protonated state of small molecules (e.g., $-\text{NH}_2$ vs. $-\text{NH}_3^+$), which critically governs the protein-ligand interactions. Such chemical nuances directly determine hydrogen-bonding patterns, charge complementarity, and binding mode stability between ligands and target proteins, making their explicit encoding essential for structure-based drug design.

Auto-Encoder

While the molecular structure effectively encodes both chemical and geometric features of molecules, the mixture of categorical atom/bond features with continuous coordinates in the molecular structure poses multi-modal challenges for diffusion based generation. Specifically, the disparate information densities across different features lead to imbalanced noise sensitivity during training. To address this, we implement an Auto-Encoder (AE) to project heterogeneous features into a homogeneous latent space $z \in \mathbb{R}^{n \times d}$. Then the diffusion model is solely trained on the latent vectors, avoiding feature-type-specific noise tuning. Instead of directly generating the coordinates and geometries of small molecules, we first generate the latent vector z and reconstruct \mathcal{G} via decoders to rebuild the molecule.

For a molecule with n heavy atoms, the latent vector $z_i \in \mathbb{R}^d, \forall i \in \{1, \dots, n\}$ is designed as follows:

$$z_i = f_1(x_i) + f_2(a_i, h_i, c_i) + \sum_{j=1}^n f_3(e_{ij}, i). \quad (1)$$

Here, f_1 is a neural network that utilizes an MLP to process continuous coordinates x_i . To account for the equivariant property of molecules, each molecule is centered to the origin and random rotation is applied, before being processed by f_1 . f_2 sums the outputs of three embedding layers, which handle the categorical node features a_i, h_i , and c_i , respectively. While f_3 extracts bond features by carrying out element-wise multiplication of embeddings representing the bond type e_{ij} and the atom index i .

Taking the latent variable z_i as input, decoders are designed as follows to reconstruct the original features:

$$\text{Atom Decoder: } \hat{v}_i = \begin{cases} \hat{x}_i = g_1(z_i) \\ (\hat{a}_i, \hat{h}_i, \hat{c}_i) = \text{softmax}(g_2(z_i)) \end{cases} \quad (2)$$

$$\text{Bond Decoder: } \hat{e}_{ij} = \text{softmax}(g_3(z_i \odot z_j)) \quad (3)$$

Here, decoders g_1 and g_2 utilize MLPs to decode coordinates x_i and categorical node features a_i, h_i , and c_i for atom i . While g_3 decodes bond types using an MLP along with the product of two latent features z_i and z_j .

During training, the model minimizes cross-entropy loss for categorical features as a_i, h_i, c_i, e_{ij} , and L_2 loss for coordinates x_i which is equivalent to the Euclidean distance. In our experiments, the model achieves categorical accuracy exceeding 99.99% and a coordinates RMSD of less than 0.05Å, which validates the effectiveness of the proposed auto-encoder and decoders, and their ability of near-lossless molecular reconstruction.

Latent Diffusion

The latent diffusion model applied in MEVO is built on the basis of the Discrete Denoising Diffusion Probabilistic Models (D3PMs)[3], which generalize diffusion-based generative models to discrete state spaces. The discrete diffusion model defines a forward Markov process $q(z_{1:T} | z_0) = \prod_{t=1}^T q(z_t | z_{t-1})$ that progressively corrupts the discrete data $z_0 \sim q(z_0)$ into a noisy latent representation z_T . Each forward step is represented by a categorical distribution parameterized through transition matrices Q_t :

$$q(z_t | z_{t-1}) = \text{Cat}(z_t; z_{t-1}Q_t), \quad (4)$$

where $Q_t \in \mathbb{R}^{K \times K}$, and K denotes the number of discrete categories. Starting from the initial data z_0 , the marginal distribution at an arbitrary step t is given by:

$$q(z_t | z_0) = \text{Cat}(z_t; z_0Q_1Q_2 \dots Q_t) = \text{Cat}(z_t; z_0\bar{Q}_t), \quad (5)$$

where we define $\bar{Q}_t = Q_1Q_2 \dots Q_t$ as the cumulative product of transition matrices. The posterior distribution at step $t - 1$ can be expressed using Bayes’ rule as:

$$q(z_{t-1} | z_t, z_0) = \text{Cat} \left(z_{t-1}; \frac{z_t Q_t^\top \odot z_0 \bar{Q}_{t-1}}{z_0 \bar{Q}_t z_t^\top} \right). \quad (6)$$

In MEVO, a transformer denoising network $\tilde{p}_\theta(z_0 | z_t)$ is introduced to predict the original tokens z_0 given the noisy input z_t and timestep t :

$$\tilde{p}_\theta(z_0 | z_t) = \prod_{i=1}^L \text{Cat}(z_0^{(i)}; \text{softmax}(\ell_\theta(z_t, t)^{(i)})). \quad (7)$$

The one-step reverse distribution is then obtained by marginalizing over all clean tokens:

$$p_\theta(z_{t-1} | z_t) = \sum_{z_0} q(z_{t-1} | z_t, z_0) \tilde{p}_\theta(z_0 | z_t). \quad (8)$$

Post-processing

The generated molecular conformation usually does not fall into a local minimum, as we do not optimize energies in the training processes. To address this, we apply a relaxation process to refine the generated conformations with molecular mechanics force fields.

Through the analysis of conformational variations across 1,000 generated molecules by comparing structures before and after relaxation, we observe an average RMSD of 0.7Å. While this deviation is non-negligible, it remains sufficiently low to preserve conformational distinctions between local energy minima. Though it might be beneficial to incorporate energy-based losses in the training processes for improving the precision of generated coordinates, we deliberately avoid this complexity. Instead, using a brief post-processing workflow of relaxation to achieve energy-minimized conformations with minimal computational overhead. Experimental results demonstrate that post-relaxation molecules maintain strong target binding.

Conditional Generation

The generative diffusion model provides a sound foundation for generating various molecule candidates, but it is often inadequate to use unconditionally generated molecules for drug discovery purpose. The goal of drug discovery is to design molecules that bind to a specific target protein, hence it would be helpful to

provide the model with necessary information about the target protein, such as the structure of the binding pocket and how does the designed ligand interact with the pocket. Therefore, we have developed a method to generate molecules under specific conditions, where two types of conditions were implemented: *pharmacophore condition* and *pocket condition*.

A pharmacophore of a molecule is a collection of spatially distributed chemical features necessary for a drug molecule to bind a target. Pharmacophore hypotheses of expected molecules can be constructed by superimposing a few active compounds, or it can be inferred from the structure of the target protein pocket, which provides significant guidance for the drug design. In MEVO, the pharmacophore condition includes the categorical types of the pharmacophore features as well as the 3D coordinates of the atomic centers. Incorporating the pharmacophore condition guides the model to generate molecules with specific pharmacophores positioned in the molecular structure as expected. However, to make the generated molecule fit the target binding pocket, it is crucial to understand the relative geometry between pharmacophores and protein pockets. To this end, the pocket condition is additionally introduced, which includes a set of residue types and atom coordinates extracted from structures of target proteins.

For conditional generation, we stack the condition embedding from the pharmacophore and pocket conditions into a sequence, then concatenate such sequence with the latent vector z as the input of the transformer denoising network. In such manner, the model can effectively attend to the conditioning features while denoising the latent vector z_i of each atom in the ligand. For each pharmacophore, its 3D coordinate is projected with a multilayer perceptron (MLP) and then combined with the type embeddings, to produce a pharmacophore feature vector. Similarly, in the pocket condition, atom coordinates of each protein residue in the pocket are projected using an MLP, then combine with residue type embeddings to form a pocket feature vector.

Incorporating the pharmacophore and pocket conditions enables the model to generate molecules that fit the expected pharmacophore and the target pocket geometry. However, due to the scarcity of protein-ligand training data, the efficacy of pocket-guided generation is not as strong as pharmacophore-guided generation, which benefits from sufficiently larger amount of training data. To address this, we design a molecule evolution strategy, that bridges the pocket condition with the pharmacophore condition, and effectively enhanced the model’s capability of generating molecules that binds the target protein pocket with high affinity.

Molecule Evolution

In the process of designing molecules, it is not sufficient to simply fit the molecule to the geometry of the target protein pocket, more importantly, the molecule should also form adequate interactions with the protein pocket. To enhance model’s capability of generating high-quality small molecule candidates, we implement an evolutionary protocol to iteratively generate molecules and gradually improve their interactions with the target protein pocket during this process. The evolutionary process exquisitely connects the pocket condition with the pharmacophore condition, using a physics-inspired scoring function, to achieve automatic improvement of the generated molecules in terms of its binding affinity with the target protein.

The physics-inspired scoring function used in the evolutionary process is defined with two terms:

- Energy Term: The potential energy changes due to the binding of ligand to the target protein (ΔU), as a rough estimation of the binding energy without considering the entropic term. This term is computed as

$$\Delta U = U(P) + U(L) - U(PL), \quad (9)$$

where $U(PL)$ is the potential energy of the co-relaxed protein-ligand complex, $U(P)$ and $U(L)$ represent the potential energies of individually relaxed protein and ligand, respectively. Lower ΔU values usually refer to stronger binding between the ligand and protein.

- Interaction Term: The fulfillment of user specified interactions. This term is calculated as follows for a generated molecule:

$$\rho = \frac{\text{num. of satisfied interactions}}{\text{num. of user specified interactions}} \quad (10)$$

Higher values of ρ indicate better fulfillment of user desired interaction in the target protein pocket. This term allows for a quantitative assessment of the “satisfactory level” of the generated molecule in terms of interactions, which also leverages expert insights to optimize the efficacy of the molecular generation.

The final score is calculated as the product of these two terms: $S = -\Delta U \times \rho$. Molecular mechanics forcefields amber-ff14sb and ByteFF[66] are used for protein and ligand, respectively.

The molecular evolution process is initiated with pocket conditions only. Due to the scarcity of the high-affinity training data of the protein-ligand complex, the binding affinities of initially generated molecules are usually less satisfying. From generated molecules, the score S is calculated and used for assessing the quality of each molecule, and the seed molecules for the next round of generation will be sampled from the top-ranking molecules, which will provide additional conditions for the subsequent round of generation. To enhance the diversity of generated molecules, we categorize them by protein residues they interact with, as well as interaction types they exhibit. Molecules ranking within the top-K of any group are collected and serves as the pool of seed molecules for the next iteration. In the subsequent round of molecule generation, 0-2 seed molecules will be selected from the pool, and their pharmacophores will be extracted and used as additional auxiliary conditions. This evolutionary strategy allows MEVO to progressively refine its generated molecules without human intervention or adjustment during the process. The design of scoring function also encourages the exploration of novel interactions, especially the ones that benefit the binding affinity. Moreover, by sampling two seeds, we can merge interaction characteristics from both molecules, which effectively accelerates the evolutionary improvement of generated molecules.

Interaction Preservation

In SBDD, it is key for the designed ligands to form sufficient interactions with the protein binding pocket, such that the designed ligands can bind to the pocket with satisfying affinities. For cases with reference known binders available, such as the 5 protein targets used for illustrating MEVO’s performance on hit discovery, we expect the generated high affinity binders to retain the critical interactions observed in known binders while exploring new contact possibilities. To define these critical interactions for each target, we proceed as follows:

1. Compute the protein-ligand interaction profile for each reference binder using ProLIF [7], recording each interaction as a pair representation: (interaction type I_{type} , residue R_i), and record the occurrence of each interaction ($C_{i,r,b}$) in each reference binder B.
2. Aggregate all unique (I_{type}, R_i) pairs for a given target and calculate their frequency across reference binders.
3. Label any (I_{type}, R_i) pair occurring in more than 30% of binders as a critical interaction for that target.

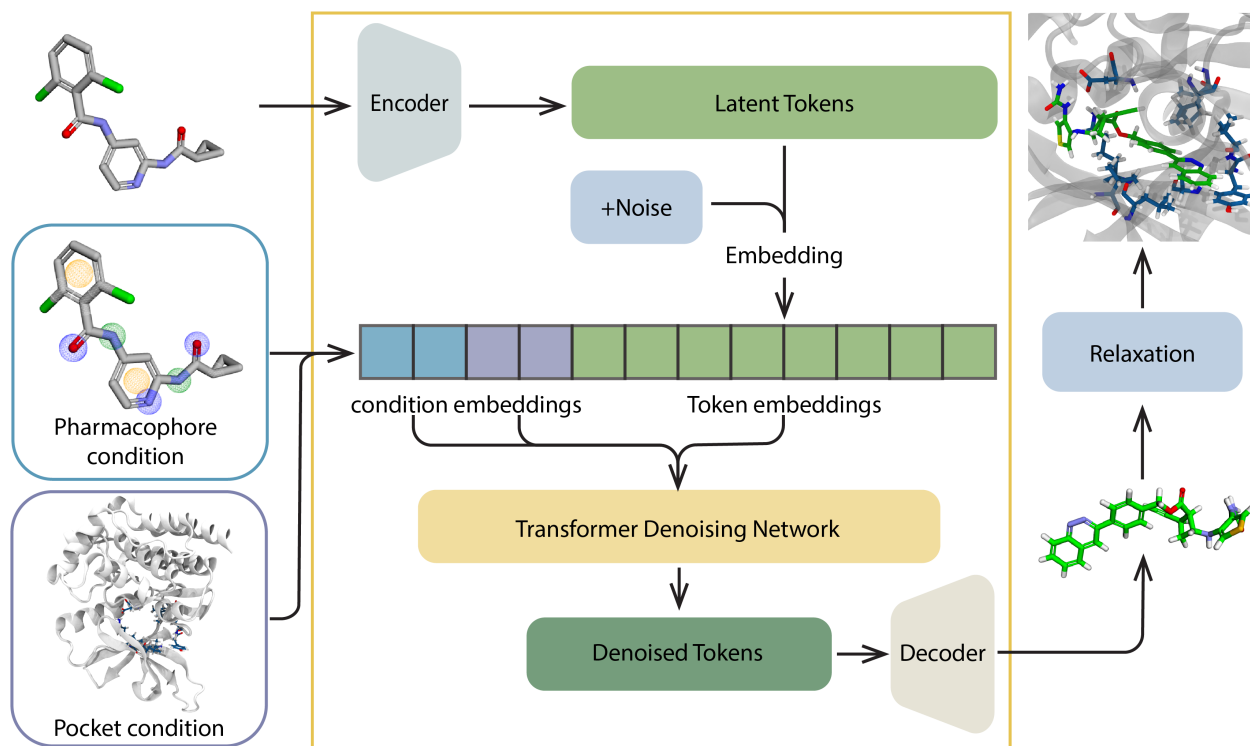
For each MEVO-generated ligand L, we similarly compute its interaction profile and record both the interaction unique representation (I_{type}, R_i) and the corresponding occurrence ($P_{i,r,l}$). We then quantify the recovery rate of critical reference interactions following the same manner defined in ref [16]. Since there are multiple reference ligands for each target, we averaged the occurrence for the same interaction among all reference ligands, and use this value for the recovery rate calculation:

$$\langle C_{i,r} \rangle = \frac{1}{|B|} \sum_{b \in B} C_{i,r,b}. \quad (11)$$

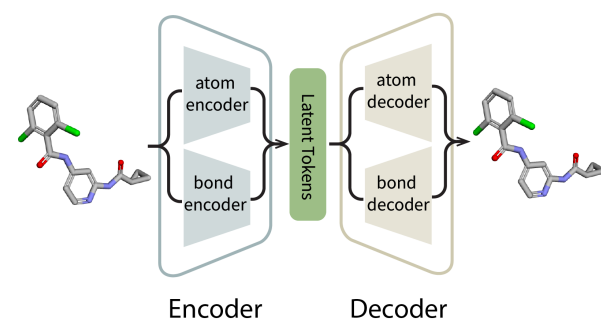
The PLIF-recovery rate for MEVO-generated ligand L is then calculated as:

$$\text{PLIF Recovery}_l = \frac{\sum_{i,r} \min(P_{i,r,l}, \langle C_{i,r} \rangle)}{\sum_{i,r} \langle C_{i,r} \rangle}. \quad (12)$$

A Latent Diffusion with Pharmacophore and Pocket Conditions for Molecule Generation



B Train High Fidelity VQ-VAE



C Evolutionary Processes

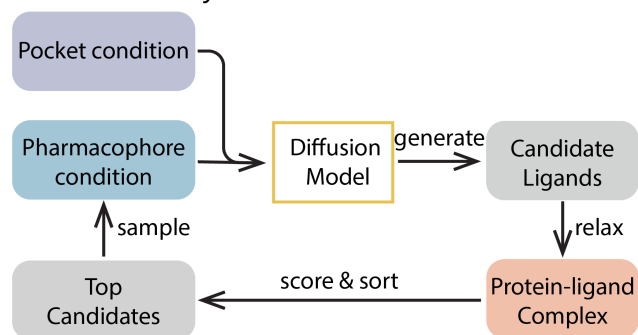


Figure 1 Overview of the MEVO model. (A) The overall architecture of MEVO model. MEVO is built on top of a discrete denoising diffusion model (yellow box), where molecules are encoded into latent tokens, and the noising/denoising processes are performed in latent space. In this process, pharmacophore and pocket conditions can be embedded as input to the denoising network, facilitating conditional generation. (B) The VQ-VAE for encoding and decoding molecules into and from latent tokens. (C) The design of evolutionary process in MEVO, which achieves automatic and iterative molecule generation–evaluation–optimization cycles.

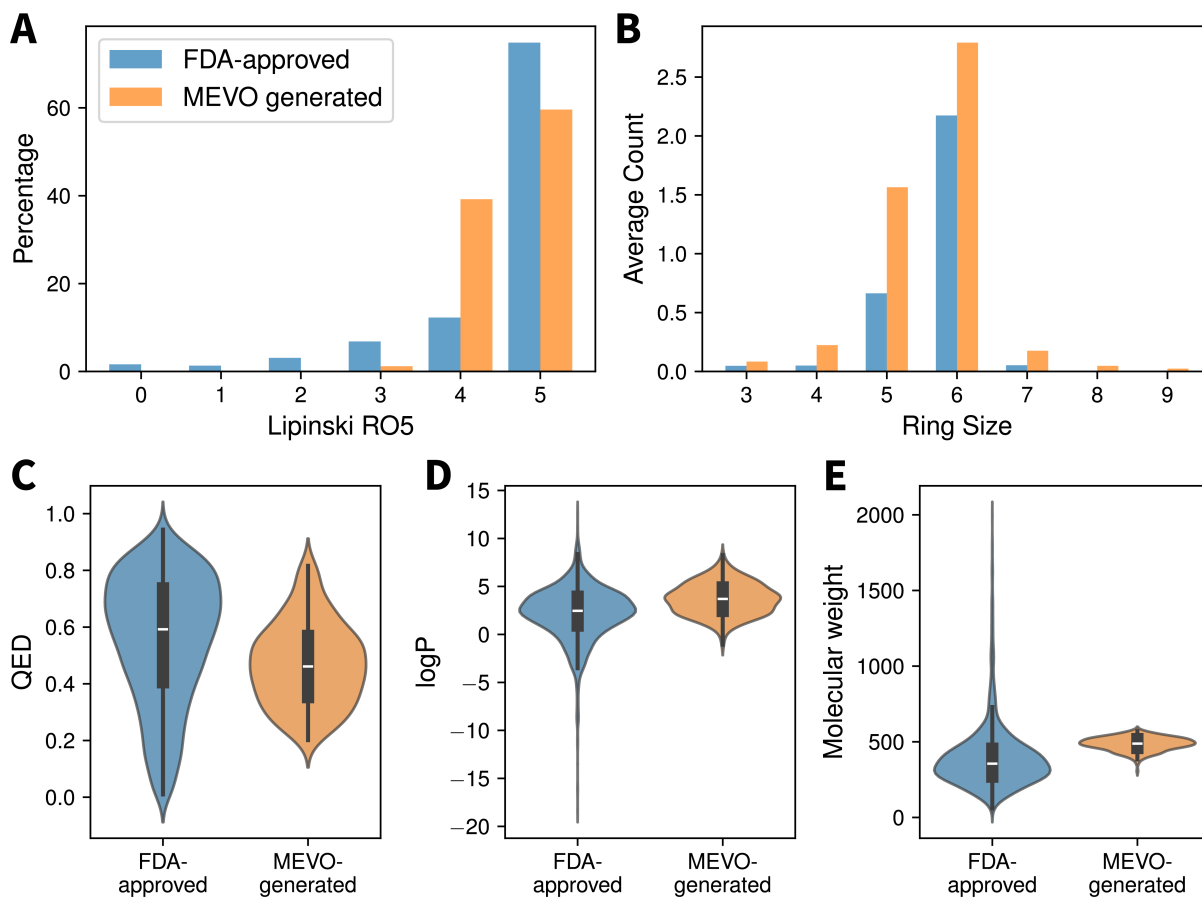


Figure 2 General properties of generated molecules in comparison with FDA approved drugs. The following metrics are included in the comparison: **(A)** Lipinski rule of 5, **(B)** distribution of counts of different ring sizes, **(C)** quantitative estimate of drug-likeness (QED), **(D)** predicted octanol-water partition coefficient (logP), **(E)** molecule weights.

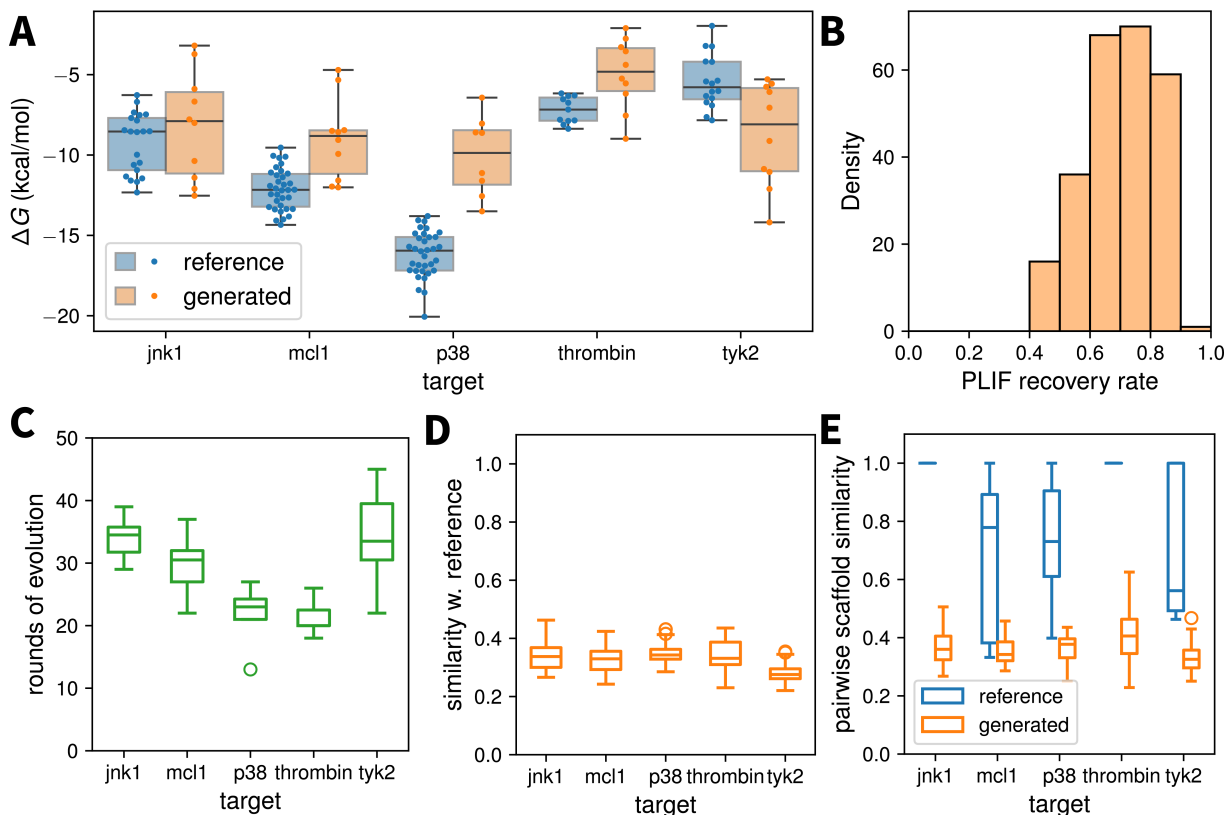


Figure 3 MEVO generated high-affinity binders to various target proteins. (A) Predicted binding affinities of generated molecules (orange) to corresponding target protein, calculated via ABFEP calculation, in comparison with predicted binding affinities of reference known binders to the same target (blue). (B) Distribution of critical interaction recovery rate of generated molecules (details in Methods). (C) Distribution of rounds of evolution for high affinity binders generated by MEVO for each target. (D) Distribution of Tanimoto similarity between generated high affinity binders and reference known binders for each target. (E) Distribution of pairwise Tanimoto similarity within Mureko scaffolds of generated high affinity binders for each target, which is plotted side-by-side with the same measurement within reference known binders for the same target.

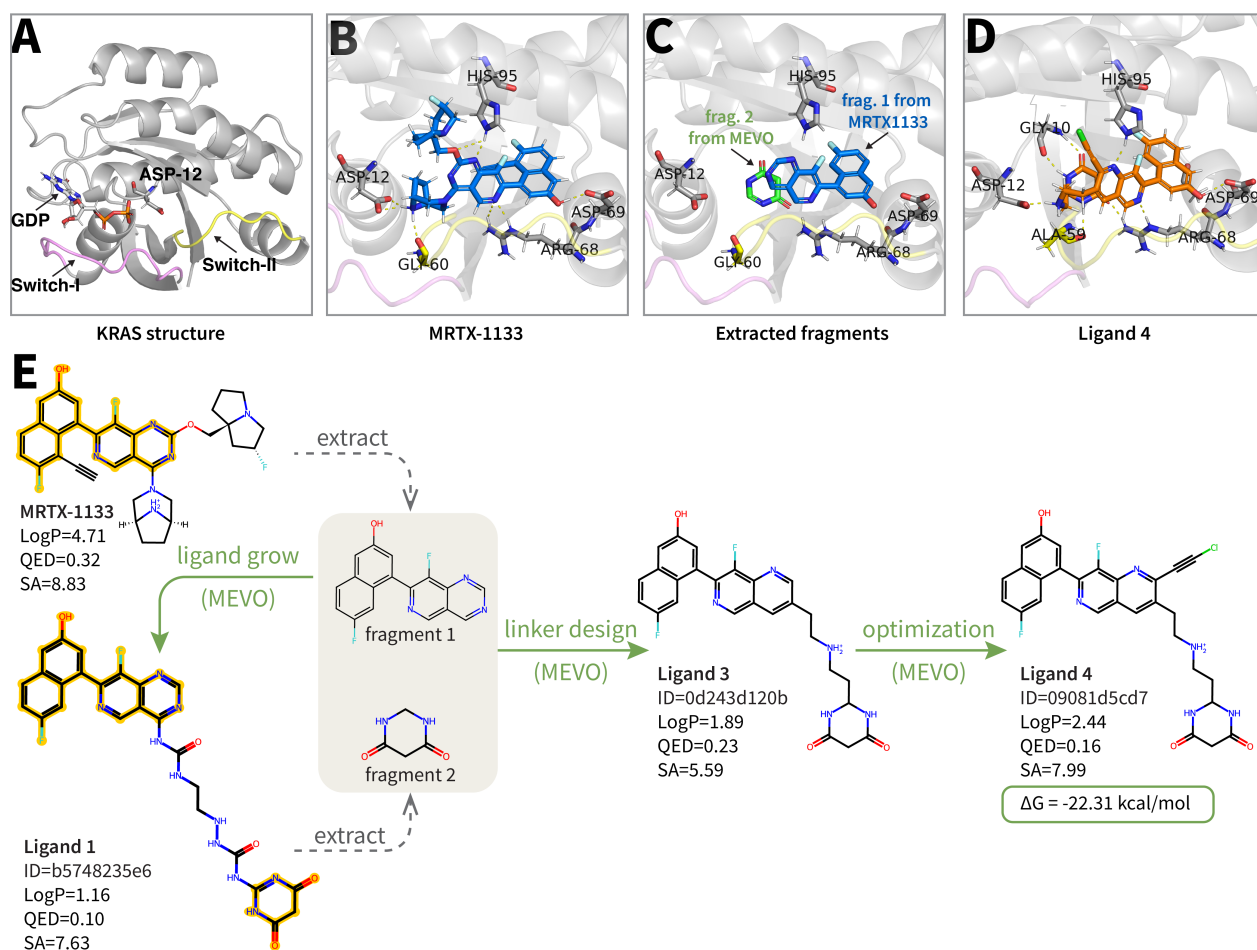


Figure 4 MEVO designs high affinity binders to KRAS^{G12D} with high versatility. **(A)** Protein structure of KRAS^{G12D} (PDB: 7T47). In its inactive state, KRAS^{G12D} binds a GDP molecule in the switch-I pocket, while some inhibitor design strategies target the switch-II pocket. **(B)** MRTX-1133 molecule in the switch-II pocket of KRAS^{G12D}. **(C)** Fragments extracted from MRTX-1133 and MEVO generated hit molecule, which are used as additional conditions in the subsequent linker design process by MEVO. **(D)** Lead molecule ligand **4** designed by MEVO. **(E)** Flowchart illustrating the design logic of ligand **4**, and how MEVO was involved in this process.

References

- [1] Leonard J Ash, Ottavia Busia-Bourdain, Daniel Okpattah, Avrosina Kamel, Ariel Liberchuk, and Andrew L Wolfe. Kras: biology, inhibition, and mechanisms of inhibitor resistance. *Current Oncology*, 31(4):2024–2046, 2024.
- [2] Kenneth Atz, Leandro Cotos, Clemens Isert, Maria Håkansson, Dorota Focht, Mattis Hilleke, David F. Nippa, Michael Iff, Jann Ledergerber, Carl C. G. Schiebroek, Valentina Romeo, Jan A. Hiss, Daniel Merk, Petra Schneider, Bernd Kuhn, Uwe Grether, and Gisbert Schneider. Prospective de novo drug design with deep interactome learning. *Nature Communications*, 15(1):3408, 2024. ISSN 2041-1723. doi: 10.1038/s41467-024-47613-w. URL <https://www.nature.com/articles/s41467-024-47613-w>.
- [3] Jacob Austin, Daniel D Johnson, Jonathan Ho, Daniel Tarlow, and Rianne Van Den Berg. Structured denoising diffusion models in discrete state-spaces. *Advances in neural information processing systems*, 34:17981–17993, 2021.
- [4] Guy W Bemis and Mark A Murcko. The properties of known drugs. 1. molecular frameworks. *Journal of medicinal chemistry*, 39(15):2887–2893, 1996.
- [5] Vincent Blay, Bhairavi Tolani, Sunita P Ho, and Michelle R Arkin. High-throughput screening: today’s biochemical and cell-based approaches. *Drug discovery today*, 25(10):1807–1821, 2020.
- [6] Albert Bou, Morgan Thomas, Sebastian Dittert, Carles Navarro, Maciej Majewski, Ye Wang, Shivam Patel, Gary Tresadern, Mazen Ahmad, Vincent Moens, Woody Sherman, Simone Sciabola, and Gianni De Fabritiis. ACEGEN: Reinforcement Learning of Generative Chemical Agents for Drug Discovery. *Journal of Chemical Information and Modeling*, 64(15):5900–5911, 2024. ISSN 1549-9596. doi: 10.1021/acs.jcim.4c00895. URL <https://doi.org/10.1021/acs.jcim.4c00895>.
- [7] Cédric Bouysset and Sébastien Fiorucci. Prolif: a library to encode molecular interactions as fingerprints. *Journal of cheminformatics*, 13(1):72, 2021.
- [8] Michael M Bronstein et al. Graphinvent: A generative model for molecular graphs. *ICLR Workshop*, 2021.
- [9] Pieter B. Burger, Xiaohu Hu, Ilya Balabin, Morné Muller, Megan Stanley, Fourie Joubert, and Thomas M. Kaiser. FEP Augmentation as a Means to Solve Data Paucity Problems for Machine Learning in Chemical Biology. *Journal of Chemical Information and Modeling*, 64(9):3812–3825, 2024. ISSN 1549-9596. doi: 10.1021/acs.jcim.4c00071. URL <https://doi.org/10.1021/acs.jcim.4c00071>.
- [10] Duanhua Cao, Geng Chen, Jiabin Jiang, Jie Yu, Runze Zhang, Mingan Chen, Wei Zhang, Lifan Chen, Feisheng Zhong, Yingying Zhang, et al. Generic protein–ligand interaction scoring by integrating physical prior knowledge and data augmentation modelling. *Nature Machine Intelligence*, 6(6):688–700, 2024.
- [11] Shicheng Chen, Odin Zhang, Chenran Jiang, Huifeng Zhao, Xujun Zhang, Mengting Chen, Yun Liu, Qun Su, Zhenxing Wu, Xinyue Wang, Wanglin Qu, Yuanyi Ye, Xin Chai, Ning Wang, Tianyue Wang, Yuan An, Guanlin Wu, Qianqian Yang, Jiean Chen, Wei Xie, Haitao Lin, Dan Li, Chang-Yu Hsieh, Yong Huang, Yu Kang, Tingjun Hou, and Peichen Pan. Deep lead optimization enveloped in protein pocket and its application in designing potent and selective ligands targeting LTK protein. *Nature Machine Intelligence*, 7(3):448–458, 2025. ISSN 2522-5839. doi: 10.1038/s42256-025-00997-w. URL <https://www.nature.com/articles/s42256-025-00997-w>.
- [12] Wei Chen, Di Cui, Steven V Jerome, Mayako Michino, Eelke B Lenselink, David J Huggins, Alexandre Beutrait, Jeremie Vendome, Robert Abel, Richard A Friesner, et al. Enhancing hit discovery in virtual screening through absolute protein–ligand binding free-energy calculations. *Journal of Chemical Information and Modeling*, 63(10):3171–3185, 2023.
- [13] Hengmiao Cheng, Puhui Li, Ping Chen, Adriana Irimia, Jae Hyun Bae, Alexei Brooun, Patrick Fagan, Richard Lam, Bingzhen Lin, Jingchuan Zhang, et al. Structure-based design and synthesis of potent and selective kras g12d inhibitors. *ACS Medicinal Chemistry Letters*, 14(10):1351–1357, 2023.
- [14] Seungyeon Choi, Sangmin Seo, Byung Ju Kim, Chihyun Park, and Sanghyun Park. PIDiff: Physics informed diffusion model for protein pocket-specific 3D molecular generation. *Computers in Biology and Medicine*, 180:108865, 2024. ISSN 0010-4825. doi: 10.1016/j.compbiomed.2024.108865. URL <https://www.sciencedirect.com/science/article/pii/S0010482524009508>.
- [15] Jerome Eberhardt, Diogo Santos-Martins, Andreas F Tillack, and Stefano Forli. Autodock vina 1.2. 0: New docking methods, expanded force field, and python bindings. *Journal of chemical information and modeling*, 61(8):3891–3898, 2021.

- [16] David Errington, Constantin Schneider, Cédric Bouysset, and Frédéric A Dreyer. Assessing interaction recovery of predicted protein-ligand poses. *Journal of Cheminformatics*, 17(1):1–13, 2025.
- [17] Paul G. Francoeur, Tomohide Masuda, Jocelyn Sunseri, Andrew Jia, Richard B. Iovanisci, Ian Snyder, and David R. Koes. Three-Dimensional Convolutional Neural Networks and a Cross-Docked Data Set for Structure-Based Drug Design. *Journal of Chemical Information and Modeling*, 60(9):4200–4215, 2020. ISSN 1549-9596. doi: 10.1021/acs.jcim.0c00411. URL <https://doi.org/10.1021/acs.jcim.0c00411>.
- [18] Richard A Friesner, Jay L Banks, Robert B Murphy, Thomas A Halgren, Jasna J Klicic, Daniel T Mainz, Matthew P Repasky, Eric H Knoll, Mee Shelley, Jason K Perry, et al. Glide: a new approach for rapid, accurate docking and scoring. 1. method and assessment of docking accuracy. *Journal of medicinal chemistry*, 47(7): 1739–1749, 2004.
- [19] Richard A Friesner, Robert B Murphy, Matthew P Repasky, Leah L Frye, Jeremy R Greenwood, Thomas A Halgren, Paul C Sanschagrin, and Daniel T Mainz. Extra precision glide: Docking and scoring incorporating a model of hydrophobic enclosure for protein- ligand complexes. *Journal of medicinal chemistry*, 49(21):6177–6196, 2006.
- [20] Wenhao Gao et al. Targetdiff: Diffusion models for target-aware molecule generation. *NeurIPS*, 2022.
- [21] Jiaqi Guan, Xiangxin Zhou, Yuwei Yang, Yu Bao, Jian Peng, Jianzhu Ma, Qiang Liu, Liang Wang, and Quanquan Gu. DecompDiff: Diffusion Models with Decomposed Priors for Structure-Based Drug Design. In *Proceedings of the 40th International Conference on Machine Learning*, pages 11827–11846. PMLR, 2023. URL <https://proceedings.mlr.press/v202/guan23a.html>.
- [22] Isabella A Guedes, Felipe SS Pereira, and Laurent E Dardenne. Empirical scoring functions for structure-based virtual screening: applications, critical aspects, and challenges. *Frontiers in pharmacology*, 9:1089, 2018.
- [23] Jill Hallin, Vickie Bowcut, Andrew Calinisan, David M Briere, Lauren Hargis, Lars D Engstrom, Jade Laguer, James Medwid, Darin Vanderpool, Ella Lifset, et al. Anti-tumor efficacy of a potent and selective non-covalent krasg12d inhibitor. *Nature medicine*, 28(10):2171–2182, 2022.
- [24] Lamei Huang, Zhixing Guo, Fang Wang, and Liwu Fu. Kras mutation: from undruggable to druggable in cancer. *Signal transduction and targeted therapy*, 6(1):386, 2021.
- [25] Lei Huang, Hengtong Zhang, Tingyang Xu, and Ka-Chun Wong. MDM: Molecular Diffusion Model for 3D Molecule Generation. *Proceedings of the AAAI Conference on Artificial Intelligence*, 37(4):5105–5112, 2023. ISSN 2374-3468. doi: 10.1609/aaai.v37i4.25639. URL <https://ojs.aaai.org/index.php/AAAI/article/view/25639>.
- [26] Fergus Imrie, Thomas E. Hadfield, Anthony R. Bradley, and Charlotte M. Deane. Deep generative design with 3D pharmacophoric constraints. *Chemical Science*, 12(43):14577–14589, 2021. ISSN 2041-6539. doi: 10.1039/D1SC02436A. URL <https://pubs.rsc.org/en/content/articlelanding/2021/sc/d1sc02436a>.
- [27] John J Irwin, Khanh G Tang, Jennifer Young, Chinzorig Dandarchuluun, Benjamin R Wong, Munkhzul Khurelbaatar, Yurii S Moroz, John Mayfield, and Roger A Sayle. Zinc20—a free ultralarge-scale chemical database for ligand discovery. *Journal of chemical information and modeling*, 60(12):6065–6073, 2020.
- [28] Dejun Jiang et al. Helixdock: A large-scale docking dataset. *Scientific Data*, 2023.
- [29] Dirk Kessler, Michael Gmachl, Andreas Mantoulidis, Laetitia J Martin, Andreas Zoephel, Moriz Mayer, Andreas Gollner, David Covini, Silke Fischer, Thomas Gerstberger, et al. Drugging an undruggable pocket on kras. *Proceedings of the National Academy of Sciences*, 116(32):15823–15829, 2019.
- [30] Dirk Kessler, Andreas Bergner, Jark Böttcher, Gerhard Fischer, Sandra Döbel, Melanie Hinkel, Barbara Müllauer, Alexander Weiss-Puxbaum, and Darryl B McConnell. Drugging all ras isoforms with one pocket. *Future medicinal chemistry*, 12(21):1911–1923, 2020.
- [31] Dongsung Kim, Lorenz Herdeis, Dorothea Rudolph, Yulei Zhao, Jark Böttcher, Alberto Vides, Carlos I Ayala-Santos, Yasin Pourfarjam, Antonio Cuevas-Navarro, Jenny Y Xue, et al. Pan-kras inhibitor disables oncogenic signalling and tumour growth. *Nature*, 619(7968):160–166, 2023.
- [32] Shengchao Liu et al. G-spherenet: Geometric deep learning for affinity prediction. *Nature Communications*, 2022.
- [33] Zhihai Liu, Yan Li, Li Han, et al. Pdbbind-cn: A protein-ligand binding affinity database with a national ranking. *Nucleic Acids Research*, 43(D1):D375–D381, 2014. doi: 10.1093/nar/gku1076.

- [34] Hannes H. Loeffler, Jiazhen He, Alessandro Tibo, Jon Paul Janet, Alexey Voronov, Lewis H. Mervin, and Ola Engkvist. Reinvent 4: Modern AI-driven generative molecule design. *Journal of Cheminformatics*, 16(1):20, 2024. ISSN 1758-2946. doi: 10.1186/s13321-024-00812-5. URL <https://doi.org/10.1186/s13321-024-00812-5>.
- [35] Enamine Ltd. Enamine real database: World’s largest collection of building blocks and screening compounds, 2023. URL <https://enamine.net/compound-collections/real-compounds>.
- [36] Shuqi Lu, Lin Yao, Xi Chen, Hang Zheng, Di He, and Guolin Ke. 3D Molecular Generation via Virtual Dynamics. *Transactions on Machine Learning Research*, 2024. ISSN 2835-8856. URL <https://openreview.net/forum?id=QvipGVdE6L>.
- [37] Andreas Luttmann, Israel Cabeza de Vaca, Leonard Sparring, José Brea, Antón Leandro Martínez, Nour Aldin Kahlous, Dmytro S. Radchenko, Yurii S. Moroz, María Isabel Loza, Ulf Norinder, and Jens Carlsson. Rapid traversal of vast chemical space using machine learning-guided docking screens. *Nature Computational Science*, 5(4):301–312, 2025.
- [38] Jiankun Lyu, Sheng Wang, Trent E Balius, et al. Ultra-large library docking for discovering new chemotypes. *Nature*, 566:224–229, 2020. doi: 10.1038/s41586-019-0917-9.
- [39] Ricardo Macarron, Martyn N Banks, Dejan Bojanic, David J Burns, Dragan A Cirovic, Tina Garyantes, Darren VS Green, Robert P Hertzberg, William P Janzen, Jeff W Paslay, et al. Impact of high-throughput screening in biomedical research. *Nature reviews Drug discovery*, 10(3):188–195, 2011.
- [40] Alexander Neumann, Lester Marrison, and Raphael Klein. Relevance of the trillion-sized chemical space “explore” as a source for drug discovery. *ACS Medicinal Chemistry Letters*, 14(4):466–472, 2023. doi: 10.1021/acsmchemlett.3c00021.
- [41] Ruth Nussinov and Hyunbum Jang. Direct k-ras inhibitors to treat cancers: progress, new insights, and approaches to treat resistance. *Annual Review of Pharmacology and Toxicology*, 64(1):231–253, 2024.
- [42] Tatu Pantzar. The current understanding of kras protein structure and dynamics. *Computational and structural biotechnology journal*, 18:189–198, 2020.
- [43] Xingang Peng, Shitong Luo, Jiaqi Guan, Qi Xie, Jian Peng, and Jianzhu Ma. Pocket2Mol: Efficient Molecular Sampling Based on 3D Protein Pockets. In *Proceedings of the 39th International Conference on Machine Learning*, pages 17644–17655. PMLR, 2022. URL <https://proceedings.mlr.press/v162/peng22b.html>.
- [44] Xingang Peng, Ruihan Guo, Yan Xu, Jiaqi Guan, Yinjun Jia, Yanwen Huang, Muhan Zhang, Jian Peng, Jiayu Sun, Chuanhui Han, Zihua Wang, and Jianzhu Ma. Decipher fundamental atomic interactions to unify generative molecular docking and design. *bioRxiv*, 2024. doi: 10.1101/2024.10.17.618827. URL <https://www.biorxiv.org/content/early/2024/10/21/2024.10.17.618827>.
- [45] Xingang Peng et al. Pocket2mol: Efficient molecular sampling based on 3d protein pockets. *ICML*, 2022.
- [46] Pavel G Polishchuk, Timur I Madzhidov, and Alexandre Varnek. Estimation of the size of drug-like chemical space based on 1d and 2d molecular descriptors. *Journal of Computer-Aided Molecular Design*, 27:675–679, 2013. doi: 10.1007/s10822-013-9672-4.
- [47] Alec Radford, Jeffrey Wu, Rewon Child, et al. Language models are unsupervised multitask learners. 2019.
- [48] Robin Rombach, Andreas Blattmann, Dominik Lorenz, et al. High-resolution image synthesis with latent diffusion models. *Proceedings of the IEEE/CVF Conference on Computer Vision and Pattern Recognition (CVPR)*, pages 10684–10695, 2022.
- [49] Gregory A Ross, Chao Lu, Guido Scarabelli, Steven K Albanese, Evelyne Houang, Robert Abel, Edward D Harder, and Lingle Wang. The maximal and current accuracy of rigorous protein-ligand binding free energy calculations. *Communications Chemistry*, 6(1):222, 2023.
- [50] Chao Shen, Gaoqi Weng, Xujun Zhang, Elaine Lai-Han Leung, Xiaojun Yao, Jinping Pang, Xin Chai, Dan Li, Ercheng Wang, Dongsheng Cao, et al. Accuracy or novelty: what can we gain from target-specific machine-learning-based scoring functions in virtual screening? *Briefings in Bioinformatics*, 22(5):bbaa410, 2021.
- [51] Dharendra K Simanshu, Dwight V Nissley, and Frank McCormick. Ras proteins and their regulators in human disease. *Cell*, 170(1):17–33, 2017.

- [52] Marta M Stepniewska-Dziubinska, Piotr Zielenkiewicz, and Pawel Siedlecki. Development and evaluation of a deep learning model for protein–ligand binding affinity prediction. *Bioinformatics*, 34(21):3666–3674, 2018.
- [53] Teague Sterling and John J Irwin. Zinc 15—ligand discovery for everyone. *JCIM*, 2015.
- [54] Minyi Su, Qifan Yang, Yu Du, Guoqin Feng, Zhihai Liu, Yan Li, and Renxiao Wang. Comparative Assessment of Scoring Functions: The CASF-2016 Update. *Journal of Chemical Information and Modeling*, 59(2):895–913, 2019. ISSN 1549-9596. doi: 10.1021/acs.jcim.8b00545. URL <https://doi.org/10.1021/acs.jcim.8b00545>.
- [55] Oleg Trott and Arthur J Olson. Autodock vina: Improving the speed and accuracy of docking with a new scoring function, efficient optimization, and multithreading. *Journal of Computational Chemistry*, 31(2):455–461, 2010. doi: 10.1002/jcc.21334.
- [56] Aaron Van den Oord, Sander Dieleman, Heiga Zen, et al. Wavenet: A generative model for raw audio. *arXiv preprint arXiv:1609.03499*, 2016.
- [57] Ashish Vaswani, Noam Shazeer, Niki Parmar, Jakob Uszkoreit, Llion Jones, Aidan N Gomez, Łukasz Kaiser, and Illia Polosukhin. Attention is all you need. *Advances in neural information processing systems*, 30, 2017.
- [58] Jake Wang, Rui Qin, Mingyang Wang, Meijing Fang, Yangyang Zhang, Yuchen Zhu, Qun Su, Qiaolin Gou, Chao Shen, Odin Zhang, Zhenxing Wu, Dejun Jiang, Xujun Zhang, Huifeng Zhao, Jingxuan Ge, Zhouhui Wu, Yu Kang, Chang-Yu Hsieh, and Tingjun Hou. Token-Mol 1.0: tokenized drug design with large language models. *Nature Communications*, 16(1):4416, 2025. ISSN 2041-1723. doi: 10.1038/s41467-025-59628-y. URL <https://www.nature.com/articles/s41467-025-59628-y>.
- [59] Lingle Wang, Yujie Wu, Yuqing Deng, Byungchan Kim, Levi Pierce, Goran Krilov, Dmitry Lupyan, Shaughnessy Robinson, Markus K Dahlgren, Jeremy Greenwood, et al. Accurate and reliable prediction of relative ligand binding potency in prospective drug discovery by way of a modern free-energy calculation protocol and force field. *Journal of the American Chemical Society*, 137(7):2695–2703, 2015.
- [60] Xiaolun Wang, Shelley Allen, James F Blake, Vickie Bowcut, David M Briere, Andrew Calinisan, Joshua R Dahlke, Jay B Fell, John P Fischer, Robin J Gunn, et al. Identification of mrtx1133, a noncovalent, potent, and selective krasg12d inhibitor. *Journal of medicinal chemistry*, 65(4):3123–3133, 2021.
- [61] Kehan Wu, Yingce Xia, Pan Deng, Renhe Liu, Yuan Zhang, Han Guo, Yumeng Cui, Qizhi Pei, Lijun Wu, Shufang Xie, Si Chen, Xi Lu, Song Hu, Jinzhi Wu, Chi-Kin Chan, Shawn Chen, Liangliang Zhou, Nenghai Yu, Enhong Chen, Haiguang Liu, Jinjiang Guo, Tao Qin, and Tie-Yan Liu. Tangen: drug design with target-aware molecule generation through a chemical language model. *Nature Communications*, 15(1):9360, 2024. doi: 10.1038/s41467-024-53632-4. URL <https://doi.org/10.1038/s41467-024-53632-4>.
- [62] Yingce Xia, Kehan Wu, Pan Deng, Renhe Liu, Yuan Zhang, Han Guo, Yumeng Cui, Qizhi Pei, Lijun Wu, Shufang Xie, Si Chen, Xi Lu, Song Hu, Jinzhi Wu, Chi-Kin Chan, Shuo Chen, Liangliang Zhou, Nenghai Yu, Haiguang Liu, Jinjiang Guo, Tao Qin, and Tie-Yan Liu. Target-aware Molecule Generation for Drug Design Using a Chemical Language Model*. 2024. doi: 10.1101/2024.01.08.574635. URL <https://www.biorxiv.org/content/10.1101/2024.01.08.574635v3>.
- [63] Weixin Xie, Jianhang Zhang, Qin Xie, Chaojun Gong, Yuhao Ren, Jin Xie, Qi Sun, Youjun Xu, Luhua Lai, and Jianfeng Pei. Accelerating discovery of bioactive ligands with pharmacophore-informed generative models. *Nature Communications*, 16(1):2391, 2025.
- [64] Jun-Lin Yu, Cong Zhou, Xiang-Li Ning, Jun Mou, Fan-Bo Meng, Jing-Wei Wu, Yi-Ting Chen, Biao-Dan Tang, Xiang-Gen Liu, and Guo-Bo Li. Knowledge-guided diffusion model for 3D ligand-pharmacophore mapping. *Nature Communications*, 16(1):2269, 2025. ISSN 2041-1723. doi: 10.1038/s41467-025-57485-3. URL <https://www.nature.com/articles/s41467-025-57485-3>.
- [65] Odin Zhang, Jintu Zhang, Jieyu Jin, Xujun Zhang, RenLing Hu, Chao Shen, Hanqun Cao, Hongyan Du, Yu Kang, Yafeng Deng, Furui Liu, Guangyong Chen, Chang-Yu Hsieh, and Tingjun Hou. ResGen is a pocket-aware 3D molecular generation model based on parallel multiscale modelling. *Nature Machine Intelligence*, 5(9):1020–1030, 2023. ISSN 2522-5839. doi: 10.1038/s42256-023-00712-7. URL <https://www.nature.com/articles/s42256-023-00712-7>.
- [66] Tianze Zheng, Ailun Wang, Xu Han, Yu Xia, Xingyuan Xu, Jiawei Zhan, Yu Liu, Yang Chen, Zhi Wang, Xiaojie Wu, Sheng Gong, and Wen Yan. Data-driven parametrization of molecular mechanics force fields for expansive chemical space coverage. *Chemical Science*, 16:2730–2740, 2025. doi: 10.1039/D4SC06640E.

- [67] Hui Zhu, Jincai Yang, and Niu Huang. Assessment of the generalization abilities of machine-learning scoring functions for structure-based virtual screening. Journal of chemical information and modeling, 62(22):5485–5502, 2022.
- [68] Wonho Zhung, Hyeongwoo Kim, and Woo Youn Kim. 3D molecular generative framework for interaction-guided drug design. Nature Communications, 15(1):2688, 2024. ISSN 2041-1723. doi: 10.1038/s41467-024-47011-2. URL <https://www.nature.com/articles/s41467-024-47011-2>.